A Sensitive $SiO_2@Fe_3O_4$/GO Nanocomposite Modified Ionic Liquid Carbon Paste Electrode for the Determination of Cabergoline

Baniasadi, Mohammad*[+]
Bam University of Medical Sciences, Bam, I.R. IRAN

Maaref, Hamed*[+]
NanoBioEletrochemistry Research Center, Bam University of Medical Sciences, Bam, I.R. IRAN

Dorzadeh, Athareh
Bam University of Medical Sciences, Bam, I.R. IRAN

Mohammad Alizadeh, Parsa
Student Research Committee, School of Public Health, Bam University of Medical Sciences, Bam, I.R. IRAN

ABSTRACT: *In this study, the initial report on determining cabergoline via nanostructure-adjusted ionic liquid carbon paste electrode with aqueous solutions is described. For this purpose, an original adjusted carbon paste electrode that uses $SiO_2@Fe_3O_4$/GO nanocomposite and 1-methyl-3-butylimidazolium bromide as a binder ($SiO_2@Fe_3O_4$/GO/CPILE) was designed. Cabergoline oxidation peak at $SiO_2@Fe_3O_4$/GO/CPILE surface was 500 mV that was approximately 200 mV less compared to the oxidation potential pertaining to the CPE surface subjected to a similar state. Moreover, there was an increase in the peak current of approximately 3.0 times greater at $SiO_2@Fe_3O_4$/GO/CPILE surface in comparison to that of the CPE. The relevant linear response range and detection limit were determined as 0.07–500.0 and 0.01 μM, correspondingly. The adjusted electrode was successful in determining cabergoline within real specimens entailing adequate results.*

KEYWORDS: *Cabergoline; Carbon paste electrode; $SiO_2@Fe_3O_4$/GO nanocomposite; Ionic liquid.*

INTRODUCTION

Cabergoline, N-[3-(dimethylamino)propyl]-N-(ethylamino)carbonyl-6-(2-propenyl)-ergoline-8b-carboxamide is a derivative of ergot alkaloid that exhibits dopamine agonist behavior [1]. Evidently, it invokes long term hindrance in prolactin secretion within hyperprolactinemia patients and rats. Furthermore, it is evident that Parkinson symptoms are appeased within monkeys treated with MPTP in addition to being

***** *To whom correspondence should be addressed.*
+ E-mail: hamedmaaref@yahoo.com
1021-9986/2020/4/11-22 12/$/6.02

influential in treating Parkinson's disease [2-6]. Inadequate UV fluorescence and absorbance is displayed by cabergoline in addition to insufficient volatility and stability, thus analytical techniques, namely gas chromatographic methods and high-performance liquid chromatography using fluorescence or UV detection are not suitable for sensitive determination [7]. Numerous methods are established and approved to ascertain cabergoline e.g. electrochemical techniques, liquid chromatography-tandem mass spectrometry, and high-performance liquid chromatographic spectrophotometry electrospray ionization tandem mass spectrometry [8-12]. From the aforementioned techniques, electroanalytical techniques are defined by adequate speed, accuracy, affordable cost, and instrumental simplicity [14-22]. The cabergoline structure possesses indole moiety including a pyrrole ring and a benzene ring. Redox responses may emanate from indole derivatives [2].

The carbon paste electrodes consisting of an organic liquid and carbon particles are extensively implemented for electrochemical sensing and biosensing because of its cost-efficient trait, fabrication simplicity, and revivable surface [23-25]. Moreover, the inadequate competency of unadjusted electrodes concerning the direct electrochemical behavior of various electro-active substances has resulted in an added focus on adjusted electrodes and mediators for catalyzing electrochemical oxidation and/or reduction [26-53]. RTILs i.e. room-temperature ionic liquids containing exceptional physiochemical traits e.g. high viscosity, high thermal stability, insignificant vapor pressure, vast electrochemical windows, and great ionic conductivity are the centers of focus as an alternate binder in preparing electrochemical sensors. The fabricated ionic liquid-based carbon paste electrodes facilitate electron transfer rate in addition to enhanced selectivity and sensitivity to determine various environmental and biological species [54, 55].

A 2D substance is known as Graphene Oxide (GO) has been the center of studies due to its exceptional properties e.g. extensive specific surface area, optimal electrical conductivity, and mechanical rigidity. Moreover, various traits of functional molecules may be substantially enhanced via adsorption onto graphene support. Currently, the graphene sheet and inorganic substance combination has enabled extensive graphene utilization. GO-magnetic hybrids are fabricated for numerous uses. Iron-based spinel oxides namely, cost efficient Fe_3O_4 are subjected to researches as anode materials pertaining to electro catalysts. In addition, Coating the surface of magnetite nanoparticles with inert silica nanoparticles is a strategy to prevent aggregation of magnetite nanoparticles, improving their chemical stability, and providing better protection against toxic chemicals [56-58].

The comprehensive study of relevant literature did not highlight any investigations on simultaneously determining cabergoline electrocatalytic behavior by applying an adjusted carbon paste electrode with $SiO_2@Fe_3O_4$/GO nanocomposite and 1-methyl-3-butylimidazolium bromide as a binder ($SiO_2@Fe_3O_4$/GO/CPILE). Therefore, an adjusted electrode was fabricated whilst investigating its performance in cabergoline quantification. The final adjusted electrode was applied to determine cabergoline concentration within real specimens.

EXPERIMENTAL SECTION

Apparatus and chemicals

The electrochemical measurements were conducted using an Autolab PGSTAT 302 N (Eco Chemie, the Netherlands) potentiostat/galvanostat. The functioning state was supervised on a General Purpose Electrochemical System (GPES) software. An electrochemical system of three electrodes consisting of an optimal $SiO_2@Fe_3O_4$/GO/CPILE, a platinum wire in the role of a counter electrode and an Ag/AgCl/KCl (3.0 M) reference electrode was employed to conduct measurements. The pH values were derived via a Metrohm 710 pH meter. The required cabergoline and relevant analytical grade reagents were acquired from Merck Co. and double distilled water was used to prepare the test solutions. Orthophosphoric acid buffers and relevant salts were then assembled (pH= 2.0 to 9.0).

Preparation of $SiO_2@Fe_3O_4$/GO nanocomposite

In order to carboxylate GO, a GO aqueous suspension of 50 mL was subjected to dilution by a factor of 2 in order to achieve 2 mg mL^{-1} concentration before being bath sonicated for a period of one hour to achieve a translucent solution. chloroacetic acid ($Cl–CH_2–COOH$) (10 g) and NaOH (12 g) were also added to GO suspension and hence bath sonicated for a period of two

hours in order to transform –OH ZnSups to –COOH by conjugating acetic acid moieties resulting in G-COOH. The produced G-OOH solution was subjected to neutralization and purification through repetitive filtering and rinsing.

Approximately 0.06 grams of GO-COOH was diluted within 42 mL of water using ultrasonic irradiation (Sono swiss SW3-H, 38 kHz, Switzerland) for a period of 20 minutes. The concoction was then stirred further intensely for a period of 30 minutes under a temperature of 60 °C. In the next stage, 106.2 mg of $FeCl_3 \cdot 6H_2O$ was included whilst stirring. Upon vigorous stirring for 30 minutes at N_2 atmosphere, 57 mg of $FeSO_4 \cdot 7H_2O$ was included and stirring commenced for another 30 minutes under N_2 atmosphere. Finally, 18 mL of 6% NH_4OH aqueous solution was included in the concoction in a drop-wise manner under a temperature of 60 °C for an hour and then reacted for a further 2 hours. The N_2 atmosphere was utilized amidst reaction to avert critical oxidation. The response concoction was subjected to centrifugation using double distilled water prior to being dried. The acquired black precipitate was Fe_3O_4/GO nanocomposite which was ready to use. SiO_2@Fe_3O_4/GO nanocomposites were assembled using developing layers of silica onto Fe_3O_4/GO surface. 15 mL of ethanol, 90 mL of tetraethoxysilane (TEOS), 0.6 mL ammonium hydroxide, and 0.6 mL of water was included in a 250 mL three-neck flask under a 40 °C temperature water bath. Fe_3O_4/GO was included in the solution amidst mechanical stirring. Extraction of solution aliquots took place upon the passing of 12 hours via centrifugation and then washed using water. It was finally vacuum dried under 60 °C temperature overnight (see Fig. 1) (59).

Electrode preparation

SiO_2@Fe_3O_4/GO/CPILEs are normally assembled *via* blending 0.96grams graphite powder and 0.04 g of SiO_2@Fe_3O_4/GO nanocomposite within a mortar, about 0.03 mL ionic liquids with the addition of 0.4 mL paraffin oil to the concoction. In the next stage, the suspension was subjected to mixing for 20 minutes and the produced uniform paste was placed in a glass tube of ca. 3.4 mm i.d. × 15 cm. A copper wire is placed within the carbon paste from the opposing side to enable electrical contact. The electrode external surface was then polished using abrasive paper prior to being used.

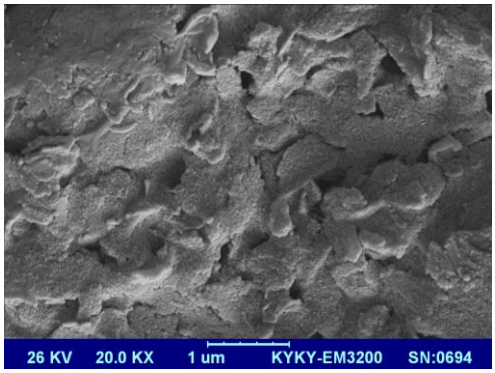

Fig. 1: SEM images of SiO_2@Fe_3O_4/GO/CPILE.

For comparison reasons, a series of SiO_2@Fe_3O_4/GO nanocomposite carbon paste electrodes lacking IL (SiO_2@Fe_3O_4/GO/CPE), IL-modified CPEs lacking SiO_2@Fe_3O_4/GO nanocomposite (CPILE), and unadjusted CPEs without IL and SiO_2@Fe_3O_4/GO nanocomposite were assembled using an identical method to the original electrode method and then tested.

The real specimens

Upon gathering, the urine specimens were preserved in a refrigerator. Before use, 10mL of every specimen was subjected to centrifugation at 2000 rpm for a quarter. Then, filtering was conducted on the supernatant using a 0.45 μm filter and various solution volumes were placed into a 25 mL flask prior to dilution to the mark via PBS of pH=7.0. The specimens were spiked using different cabergoline quantities.

The serum samples were then centrifuged prior to being filtered and diluted using PBS pH=7.0 and spiked using various quantities of the same composite.

RESULTS AND DISCUSSION

Electrochemical characterization of electrodes

$[Fe(CN)_6]^{3-/4-}$ pairs are typically used as an electrochemical probe to investigate the traits of the sensors. The SiO_2@Fe_3O_4/GO/CPILE electrochemical performance was conducted within 5.0 mM $[Fe(CN)_6]^{3-/4-}$ redox probe. According to Fig. 2, the SiO_2@Fe_3O_4/GO/CPILE redox peaks are substantially improved compared to that of the unadjusted CPE and SiO_2@Fe_3O_4/GO/CPILE. The reason can be accredited to the exceptional electron mediator property of the ILs

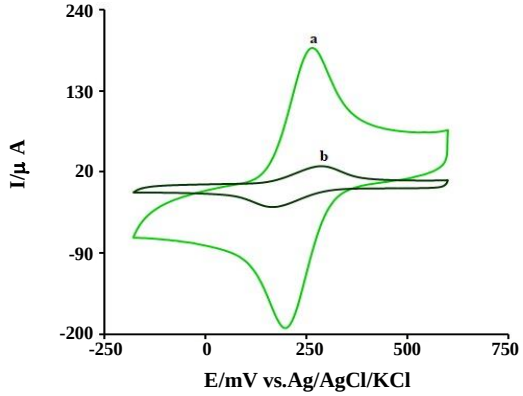

Fig. 2: CVs of a) SiO_2@Fe_3O_4/GO/CPILE and b) unmodified CPE in the presence of 5.0 mM $[Fe(CN)_6]^{3-/4-}$ containing 0.1 M KCl, respectively. In all cases, the scan rate was 50 mV/s.

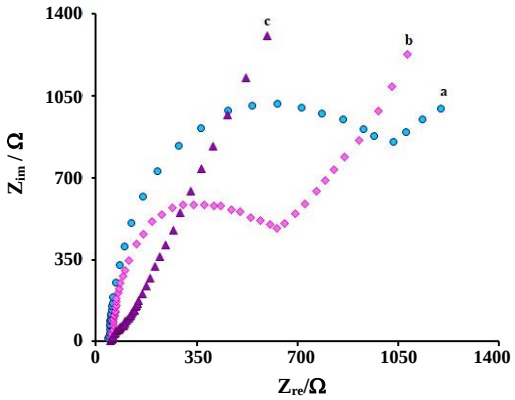

Fig. 3: EIS diagrams in 5.0 mM $[Fe(CN)_6]^{3-/4-}$ containing 0.1 M KCl at different electrode (a) CPE, (b) CPILE and (c) SiO_2@Fe_3O_4/GO/CPILE. Conditions: polarization potential: 0.15 V, frequency: 5.0×10^{-3} to 10^5 Hz. 5 M.

and the vast surface areas of the SiO_2@Fe_3O_4/GO nanocomposite whilst accelerating the transfer of electrons thus leading to the greater current reaction. The SiO_2@Fe_3O_4/GO/CPILE peak potential (ΔE_p) among the cathodic and anodic peak potential is approximately 68 mV. This value for the unadjusted CPE is 128 mV. Thus, an insignificant ΔE_p value pertaining to SiO_2@Fe_3O_4/GO/CPILE shows an expeditious and quasi reversible electron transfer scheme, proving the ability of the electrode in providing an optimal microenvironment to undertake effortless electron transfer response.

Real surface areas of the SiO_2@Fe_3O_4/GO/CPILE and CPE were acquired via CV by employing 5.0 mM $K_3Fe(CN)_6$ which acted as a probe under various scan rates. The Randles-Sevcik formulation was used for the reversible procedure:

$$I_p = \pm\left(2.69\times10^5\right)n^{3/2}AD^{1/2}Cv^{1/2} \quad (1)$$

Such that I_{pa} (A) denotes anodic peak current and *n* represents electron transfer number. A denotes electrode *D* surface area, *D* denotes diffusion coefficient, *C* is the $K_3Fe(CN)_6$ concentration in (mol cm^{-3}), v represents scan rate. In the case that 5.0 mM $K_3Fe(CN)_6$ within 0.1 M KCl electrolyte where n = 1 and D = 7.6×10^{-6} cm^2/s, thus from the $I_{pa} - v^{1/2}$ relation slope, real surface areas are derived. The findings indicate that for the CPE, the electron surface area is 0.1719 cm^2 and for the SiO_2@Fe_3O_4/GO/CPILE, the surface area is 0.2647 cm^2. Hence, the surface areas for SiO_2@Fe_3O_4/GO/CPILE were 1.54 times greater compared to that of the CPE. Although, the analyte peak current increase at SiO_2@Fe_3O_4/GO/CPILE surface does not only result from the surface area the IL and SiO_2@Fe_3O_4/GO nanocomposite synergic impact on cabergoline oxidation is also influential.

EIS is considered an influential probe in determining the adjusted electrode's electron transfer traits. Fig. 3 shows the CPE, CPILE and SiO_2@Fe_3O_4/GO/CPILE Nyquist plots within 5.0 mM $[Fe(CN)_6]^{3-/4-}$ possessing 0.1 M KCl. The electrode surface electron transfer resistance i.e. R_{ct} is equal to EIS semicircle diameter which may be useful in describing the electrode's interface characteristics. A large semicircle of about 1036 Ω (R_{ct}) diameter was evident at the bare CPE (curve a) which shows a significantly low electron transfer rate among the CPE and electrochemical probe $[Fe(CN)_6]^{3-/4-}$. Moreover, in regard to the Nyquist plots, there were significantly smaller semicircle diameters that were approximately 706 Ω (curve b) which shows the CPE electrode conductivity promoted by the IL. Upon the addition of the SiO_2@Fe_3O_4/GO nanocomposite to the CPILE electrode, there was a reduction of the R_{ct} down to 82 Ω. The figure shows the impedance variances at the adjusted electrodes which validates the exceptional conductivity of the SiO_2@Fe_3O_4/GO nanocomposite which expedites electron transfer. The evident impedance variances stemmed from the IL and SiO_2@Fe_3O_4/GO nanocomposite synergistic impact in $[Fe(CN)_6]^{3-/4-}$ electrochemical response as well as the surface area traits.

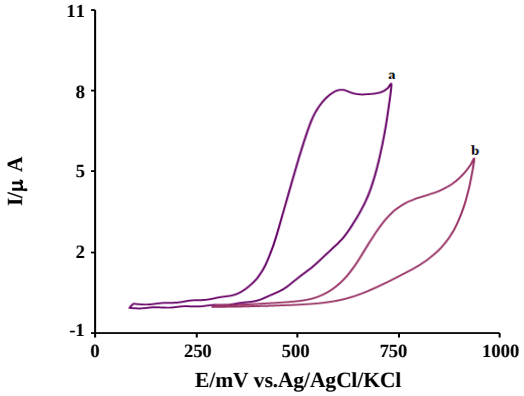

Fig. 4: CVs of a) $SiO_2@Fe_3O_4$/GO/CPILE and b) unmodified CPE in the presence of 100.0 µM cabergoline at a pH 7.0, respectively. In all cases the scan rate was 50 mV/s.

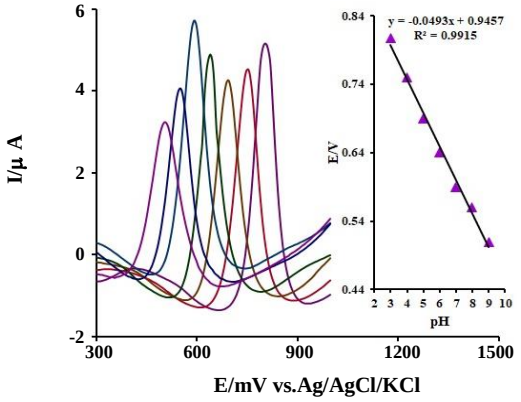

Fig. 5: Effect of pH on the peak current for the oxidation of cabergoline (70.0 µM); pH= 3-9. Scan rate: 50 mV/s. Inset: Plot of peak potential vs. pH.

Oxidation of cabergoline at the surface of the $SiO_2@Fe_3O_4$/GO/CPILE

Cabergoline activities depend mostly on the pH solution whilst this is not the case concerning Fc/Fc^+. Thus, pH optimization is a vital stage. Hence, CV investigations took place utilizing 0.1 PBS solutions of different pH values within the 2.0 to 9.0 range. The tests showed cabergoline electrocatalytic oxidation was more optimal with neutral pH values as exhibited via moderate increments and decrements of the cathodic and anodic peak currents. According to the data, optimal pH was 7.0 thus it was employed for all tests.

Fig. 4 shows the cyclic voltammetric reactions emanating from 100.0 µM cabergoline electrochemical oxidation at $SiO_2@Fe_3O_4$/GO/CPILE (curve a) and bare CPE (curve b) surface. The relevant anodic peak potential for cabergoline oxidation at $SiO_2@Fe_3O_4$/GO/CPILE was approximately 550 mV whereas it was 750 mV for the unadjusted CPE. Likewise, when comparing cabergoline oxidation at $SiO_2@Fe_3O_4$/GO/CPILE and unadjusted CPE, it is evident that there is a substantial enhancement in terms of anodic peak current at $SiO_2@Fe_3O_4$/GO/CPILE in relation to the acquired value for the unadjusted CPE. Essentially, the findings clarify the cabergoline oxidation signal is improved by ionic liquids and the $SiO_2@Fe_3O_4$/GO nanocomposite.

pH effect

The pH effect of the existing electrolyte on the potentials and anodic peak currents was studied to obtain the optimal shape and peak current. Herein, differential pulse voltammetric evaluation was performed on several buffered solutions within the 3.0 to 9.0 pH range pertaining to the cabergoline solutions. Fig. 5 shows that in the case that the pH is enhanced to 5.0 from 3.0, there was a reduction in current and then an enhancement in peak current up to 0.7 before another reduction.

Thus, the optimal pH was 7.0. Hence, pH=7.0 and 0.1 M phosphate buffer solution was chosen as the supplementary electrolyte for the voltammetric analysis. Cabergoline $E_{p,a}$ exhibits a linear relationship with buffer solution pH (as shown in Fig. 5) for the equation (2):

$$E_{p,a}(V) = -0.0493pH + 0.9457 \left(R^2 = 0.9915\right) \quad (2)$$

Regarding the cabergoline slope of -50.0 mV/pH, equal electron and proton quantities are contributing to the electrodes' reactions. Scheme 1 presents the assumed cabergoline oxidation technique.

Scan rate effect

The potential scan rate impact on cabergoline oxidation current is investigated (Fig. 6). The findings indicate that when the potential scan rate is enhanced, there is an enhancement in peak current. Additionally, the oxidation procedure is diffusion-controlled which is derived from linear reliance of anodic peak current (I_p) on potential scan rate square root ($\nu^{1/2}$) across an extensive 10 -600 mV/s range.

Chronoamperometric studies

Cabergoline chronoamperometric measurements were conducted at $SiO_2@Fe_3O_4$/GO/CPILE via selecting

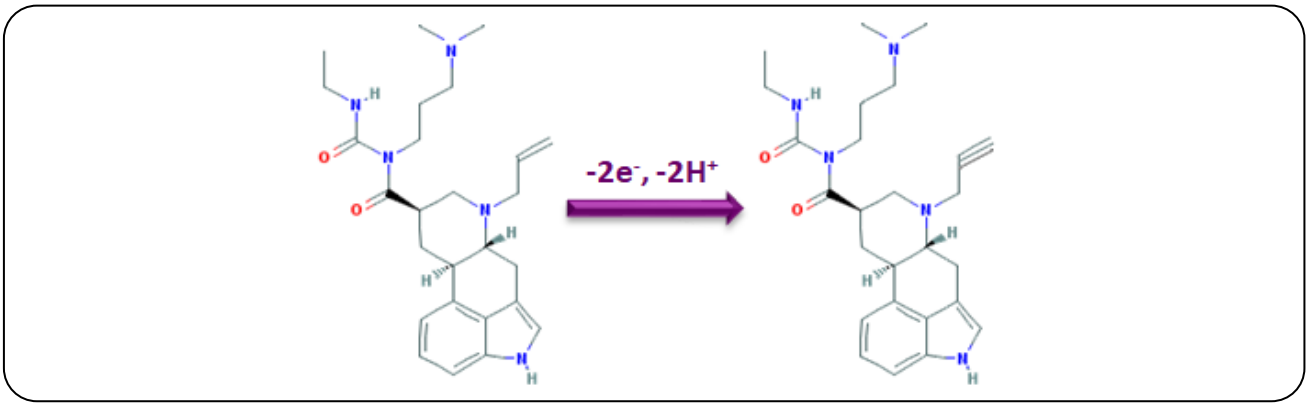

Scheme 1. Electro-oxidation mechanism of cabergoline at SiO_2@Fe_3O_4/GO/CPILE.

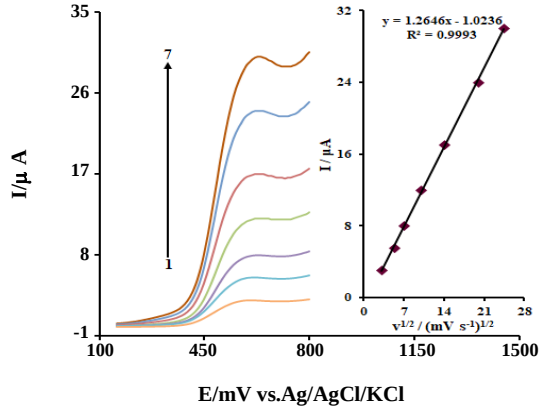

Fig. 6: LSVs of SiO_2@Fe_3O_4/GO/CPILE in 0.1 M PBS (pH 7.0) containing 200.0 μM cabergoline at various scan rates; numbers 1-7 correspond to 10, 30, 50, 100, 200, 400 and 600 mV/s, respectively. Inset: Variation of anodic peak current vs. square root of scan rate.

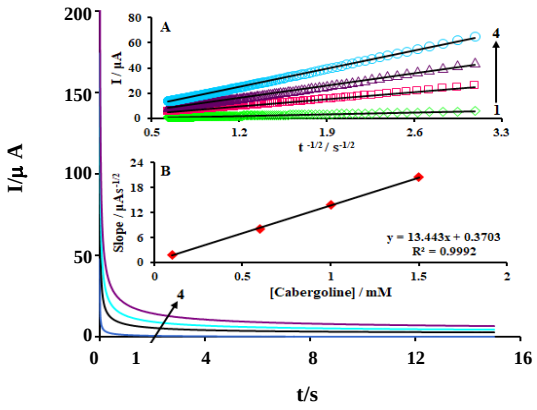

Fig. 7. Chronoamperograms obtained at SiO_2@Fe_3O_4/GO/CPILE in 0.1 M PBS (pH 7.0) for different concentrations of cabergoline. The numbers 1–4 correspond to 0.1, 0.6, 1.0, and 1.5 mM of cabergoline. Insets: (A) Plots of I vs. $t^{-1/2}$ obtained from chronoamperograms 1–4. (B) Plot of the slope of the straight lines against cabergoline concentration.

working electrode potential at 0.6V pertaining to different cabergoline concentrations within PBS pH=7.0 as shown in Fig. 7. In the case of electroactive materials e.g. cabergoline with D as diffusion coefficient, the current pertaining to electrochemical response at mass transport limited state is presented via Cottrell equation [60].

$$I = nFAD^{1/2}C_b\pi^{-1/2}t^{-1/2} \quad (3)$$

Such that D and C_b denote diffusion coefficient (cm^2/s) and bulk concentration (mol cm^{-3}), correspondingly. The I vs. $t^{-1/2}$ empirical plots were used including optimal fits for various cabergoline concentrations as shown in Fig. 7A. The resulting straight-line slopes are drawn against cabergoline concentrations as shown in Fig. 7B. The mean value of D derived from the Cottrell equation and the resulting slope was 1.9×10^{-6} cm^2/s

The calibration curve and limit of detection

Cabergoline oxidation peak current at the adjusted electrode surface may be utilized to ascertain cabergoline within a solution. Thus, DPV tests were conducted for various cabergoline concentrations as shown in Fig. 8. Cabergoline oxidation peak currents at unadjusted electrode surface corresponded to cabergoline concentrations within the 0.07 to 500.0 μM range. The Cabergoline detection limit was 0.01 μM.

A comparison is presented between SiO_2@Fe_3O_4/GO/CPILE analytical performances resulting from this study with the sensors contributing to

Table 1: Comparison of the efficiency of different methods used in detection of cabergoline.

Method	Modifier	LOD	LDR	Ref
Voltammetry	Maghemite (γ-Fe_2O_3) nanoparticles	0.03 µM	0.1-0.35 µM	[2]
Voltammetry	Graphene	5.441 ng mL^{-1}	0.2-5.2 µg mL^{-1}	[12]
Voltammetry	Nickel nanoparticles	2.0 µM	5.0-2700.0 µM	[61]
Voltammetry	Graphene oxide/ZnO nanocomposite	0.45 µM	1.0-200.0 µM	[62]
Liquid chromatography–mass spectrometry	-	2 pg/ml	5-250 pg/ml	[63]
High-performance liquid chromatographic	-	0.05 µg mL^{-1}	0.1–4 µg mL^{-1}	[64]
Voltammetry	SiO_2@Fe_3O_4/GO nanocomposite	0.01 µM	0.07-500.0 µM	This work

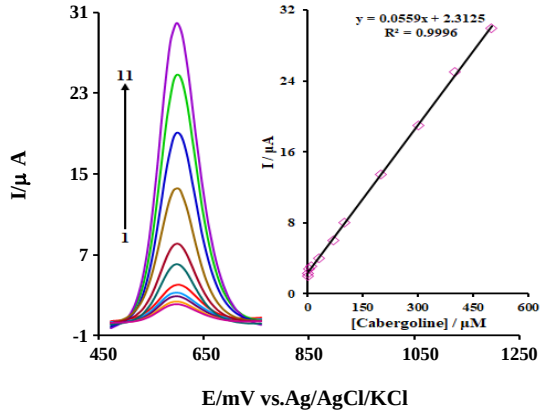

Fig. 8: DPVs of SiO_2@Fe_3O_4/GO/CPILE in 0.1 M PBS (pH 7.0) containing different concentrations of cabergoline. Numbers 1-11 correspond to 0.07, 1.0, 5.0, 10.0, 30.0, 70.0, 100.0, 200.0, 300.0, 400.0 and 500.0 µM of cabergoline. Inset: plots of the electrocatalytic peak current as a function of cabergoline concentration in the range of 0.07 to 500.0 µM.

cabergoline evaluation (2, 13, 57-60) (Table 1). The recommended approach did not exhibit a favorable detection limit compared to prior approaches mentioned in the literature apart from the method presented in ref (59). The results of this study compared to ref (59) are superior in terms of simplicity and not requiring pretreatment procedures. Thus, SiO_2@Fe_3O_4/GO/CPILE exhibits optimal analytic performance to determine cabergoline in regards to the significantly low detection limit, extensive linear dynamic range, exceptional reproducibility, and repeatability as well as higher sensitivity in comparison to the aforementioned approaches in the literature.

Interference and repeatability studies

The effect of different materials as composites potentially involved in determining cabergoline is investigated at optimal circumstances with 20.0 µM cabergoline at pH= 7.0. The possibly contributing materials were selected among a set of materials typically observed with cabergoline within biological and/or pharmaceutical liquids. The limit of tolerance was determined as the maximal concentrations of contributing materials which led to an error that was less than ±6% in determining cabergoline. Based on the findings, urea, saturated starch solution, folic acid (vitamin B_9), glycine, phenylalanine, methionine, alanine, Cl^- or F^-, Fe^{3+},CO_3^{2-}, NH_4^+, Fe^{2+}, Al^{3+}, SO_4^{2-}, Mg^{2+}, ethanol, methanol, citric acid, fructose, lactose, sucrose, and glucose were not involved in determining cabergoline.

In the vicinity of cabergoline, voltammograms were documented upon potential cycling of 20 repetitions at 50 mV/s scan rate. Based on the outcomes, there were no changes in terms of peak potentials apart from a decrease of less than 2.43%. The results validated the greater sensitivity and decreased fouling impact of SiO_2@Fe_3O_4/GO/CPILE in regard to cabergoline and relevant oxidation byproducts.

Real samples analysis

In order to validate the competency of the adjusted electrode to implement in real analytical cases, it was utilized to determine cabergoline within urine specimens and human blood serum. The findings for cabergoline concentration within real samples are shown in Table 2. Based on this table, there were adequate recovery results achieved for cabergoline. Cabergoline reproducibility is denoted in terms of the relative standard deviation i.e. RSD.

CONCLUSIONS

The adjusted paste electrode was developed *via* blending graphite, SiO_2@Fe_3O_4/GO nanocomposite,

Table 2: The application of SiO_2@Fe_3O_4/GO/CPILE for concurrent determination of cabergoline in human blood serum and urine samples (n=5). All concentrations are in µM.

Sample	Spiked	Found	Recovery (%)	R.S.D. (%)
Human blood serum	0	-	-	-
	5.0	4.9	98.0	2.4
	10.0	10.1	101.0	1.7
	15.0	15.5	103.3	3.4
	20.0	19.8	99.0	1.9
Urine	0	-	-	-
	7.5	7.7	102.7	3.2
	12.5	12.3	98.4	3.1
	17.5	17.1	97.7	1.7
	22.5	22.6	100.4	1.2

paraffin (SiO_2@Fe_3O_4/GO/CPILE) and ionic liquids. By making the most of the structural benefits of SiO_2@Fe_3O_4/GO nanocomposite as well as the favorable IL conductivity, the recommended sensor displayed exceptional electrochemical behavior in regard to cabergoline. The electrochemical activity of cabergoline in regard to the adjusted electrode was subjected to meticulous examination including the calculation of electrochemical parameters. This electrochemical procedure exhibits the trait of a diffusion control system and is quasi reversible. This recommended sensor exhibited favorable properties, namely long-term stability, low detection limit, extensive linear calibration range, high sensitivity, affordable cost, and simplicity. Lastly, the fabricated sensor was implemented to determine cabergoline within real specimens and sufficient recoveries were acquired.

Received : Apr. 16, 2019 ; Accepted :May 20, 2019

REFERENCES

[1] Chiba S., Numakawa T., Ninomiya M., Shin Yoon H., Kunugi H., Cabergoline, A Dopamine Receptor Agonist, Has an Antidepressant-Like Property and Enhances Brain-Derived Neurotrophic Factor Signaling, *Psychopharmacology*, **211**: 291-301 (2010).

[2] Hasanpour F., Taei M., Banitaba S.H., Heidari M., Template Synthesis of Maghemite Nanoparticle in Carboxymethyl Cellulose and its Application for Electrochemical Cabergoline Sensing, *Mater. Sci. Eng. C*, **76**: 88-93 (2017).

[3] Ogul H., Kaya S., Ogul Y., Transient Splenial Lesion of the Corpus Callosum after Cabergoline Treatment, *World Neurosurg.*, **114**: 257-258 (2018).

[4] Saad A.S., Aziz Mohamed K.A., Diosmin Versus Cabergoline for Prevention of Ovarian Hyperstimulation Syndrome, *Middle East Fertil. Soc. J.*, **22**: 206-210 (2017).

[5] Oberhaus E.L., Thompson D.L., Pham C.K., Valencia N.A., Seasonal Assessment of Duration of Prolactin Suppression Following Cabergoline Treatment In Mares: Unstimulated Versus Sulpiride and Thyrotropin-Releasing Hormone-Stimulated Responses, *J. Equine Vet .Sci.*, **58**: 13-19 (2017).

[6] A. Mogheiseh A., Mosavi Ghiri M.J., Bandarian E., The Clinical Follow-Up of Estradiol Benzoate Priming During Induction of Estrus with Cabergoline in Dogs, *Top Companion Anim. Med.*, **32**: 16-19 (2017).

[7] Pianezzola E., Bellotti V., Croix R.L., Strolin Benedetti M., Determination of Cabergoline in Plasma and Urine by High-Performance Liquid Chromatography with Electrochemical Detection, *J. Chromatogr. A*, **574**: 170-174 (1992).

[8] Onal A., Sagirli O., Sensoy D., Selective LC Determination of Cabergoline in the Bulk Drug and in Tablets: in Vitro Dissolution Studies, *Chromatographia*, **65**: 561-567 (2007).

[9] Kimball B.A., De Liberto T.J., Johnston J.J., Determination of Cabergoline by Electrospray Ionization Tandem Mass Spectrometry: Picogram Detection Via Column Focusing Sample Introduction, *Anal. Chem.*, **73**: 4972-4976 (2001).

[10] Igarashi K., Hotta K., Kasuya F., Abe K., Sakoda S., Determination of Cabergoline and L-Dopa in Human Plasma Using Liquid Chromatography-Tandem Mass Spectrometry, *J. Chromatogr. B*, **792**: 55-61 (2003).

[11] Arabzadeh H., Shahidi M., Foroughi M.M., Electrodeposited Polypyrrole Coatings on Mild Steel: Modeling the EIS Data with a New Equivalent Circuit and the Influence of Scan Rate and Cycle Number on the Corrosion Protection, *J. Electroanal. Chem.*, **807**: 163-173 (2017).

[12] Jain R., Sinha A., A Graphene Based Sensor for Sensitive Voltammetric Quantification of Cabergoline, *J. Electrochem. Soc.*, **161**: H314-H320 (2014).

[13] Soltani Nejad M., Shahidi Bonjar G.H., Khatami M., Amini A., Aghighi S., *In Vitro* and *In Vivo* Antifungal Properties of Silver Nanoparticles Against Rhizoctonia Solani, a Common Agent of Rice Sheath Blight Disease, *IET Nanobiotechnol.*, **11**: 236-240 (2017).

[14] Foroughi M.M., Jahani Sh., Hasani Nadiki H., Lanthanium Doped Fern-Like CuO Nanoleaves/Mwcnts Modified Glassy Carbon Electrode for Simultaneous Determination of Tramadol and Acetaminophen, *Sens. Actuators B*, **285**: 562-570 (2019).

[15] Darroudi A., Eshghi H., Rezaeian S., Chamsaz M., Bakavoli M., Haghbeen K., Hosseiny A., A Novel Carbon Paste Electrode for Potentiometric Determination of Vanadyl Ion, *Iran. J. Chem. Chem. Eng. (IJCCE)*, **34**: 89-94 (2015).

[16] Azizi Z. Pourseyedi S., Khatami M., Mohammadi H., Stachys Lavandulifolia and Lathyrus sp. Mediated for Green Synthesis of Silver Nanoparticles and Evaluation its Antifungal Activity Against Dothiorella Sarmentorum, *J. Cluster Sci.*, **27**: 1613-1628 (2016)

[17] Foroughi M.M., Ranjbar M., Microwave-Assisted Synthesis and Characterization Photoluminescence Properties: a Fast, Efficient Route to Produce ZnO/GrO Nanocrystalline, *J. Mater. Sci.*, **28**: 1359-1363 (2017).

[18] Naddaf E., Abedi M.R., Zabihi M.S., Imani A., Electrocatalytic Oxidation of Ethanol And Ethylene Glycol onto Poly (O-Anisidine)-Nickel Composite Electrode, *Iran. J. Chem. Chem. Eng.(IJCCE)*, **36**: 59-70 (2018).

[19] Soltani Nejad, M., Khatami, M., Shahidi Bonjar, G.H., Extracellular Synthesis Gold Nanotriangles Using Biomass of Streptomyces Microflavus, *IET Nanobiotechnol.*, **10**: 33-38 (2016).

[20] Hajializadeh A., Tajik S., Jahani Sh., Beitollahi H., Synergic Effect of Cu (II) Nanocomplex for the Fabrication of Highly Sensitive Voltammetric Sensor for Levodopa Determination, *Anal. Bioanal. Electrochem.*, **10**: 292-301 (2018).

[21] Asaadi N., Parhizkar M., Mohammadi Aref S., Bidadi, H., The Role of Polypyrrole in Electrical Properties of ZnO-Polymer Composite Varistors, *Iran. J. Chem. Chem. Eng.(IJCCE)*, **36**: 65-72 (2017).

[22] Salajegheh M., Ansari M., Foroghi M.M., Kazemipour M., Computational Design as a Green Approach for Facile Preparation of Molecularly Imprinted Polyarginine-Sodium Alginate-Multiwalled Carbon Nanotubes Composite Film on Glassy Carbon Electrode for Theophylline Sensing, *J. Pharm. Biomed. Anal.*, **162**: 215-224 (2019).

[23] Arefi Nia N., Foroughi M.M., Jahani Sh., Shahidi Zandi M., Rastakhiz N., Fabrication of a New Electrochemical Sensor for Simultaneous Determination of Codeine and Diclofenac Using Synergic Effect of Feather-Type La3+-ZnO Nano-Flower, *J. Electrochem. Soc.*, **166**: B489-B497 (2019).

[24] Foroughi M.M., Jahani Sh., Rajaei M., Facile Fabrication of 3D Dandelion-Like Cobalt Oxide Nanoflowers and Its Functionalization in the First Electrochemical Sensing of Oxymorphone: Evaluation of Kinetic Parameters at The Surface Electrode, *J. Electrochem. Soc.*, **166**: B1300-B1311 (2019).

[25] Vakili Fathabadi V., Hashemipour Rafsanjani H., Foroughi M.M., Jahani Sh., Arefi Nia N., Synthesis of Magnetic Ordered Mesoporous Carbons (OMC) as an Electrochemical Platform for Ultrasensitive and Simultaneous Detection of Thebaine and Papaverine, *J. Electrochem. Soc.*, **167**: 027509 (2020).

[26] Gupta V.K., Agarwal S., Singhal B., Recent Advances on Potentiometric Membrane Sensors for Pharmaceutical Analysis, *Comb. Chem. High Throughput Screen*, **14**: 284-302 (2011).

[27] Gupta V.K., Sethi B., Sharma R.A., Agarwal S., Bharti A., Mercury Selective Potentiometric Sensor Based on Low Rim Functionalized Thiacalix [4] Arene as a Cationic Receptor, *J. Mol. Liq.*, **177**: 114-118 (2013).

[28] Sheibani N., Kazemipour M., Jahani Sh., Foroughi M.M., A Novel Highly Sensitive Thebaine Sensor Based on MWCNT and Dandelionlike CO_3O_4 Nanoflowers Fabricated *via* Solvothermal Synthesis, *Microchem. J.*, **149**: 103980 (2019).

[29] Vgupta V.K., Ganjali M.R., Norouzi P., Khani H., Nayak A., Agrawal S., Electrochemical Analysis of Some Toxic Metals and Drugs by Ion Selective Electrodes, *Crit. Rev. Anal. Chem.*, **41**: 282-313 (2011).

[30] Srivastava S.K., Gupta V.K., Jain S., Determination of Lead Using Poly (Vinyl Chloride) Based Crown Ether Membrane, *Analyst*, **120**: 495-498 (1995).

[31] Yan S.R., Foroughi M.M., Safaei M., Jahani Sh., Ebrahimpour N., Borhani F., Rezaei Zade Baravati Z., Aramesh-Boroujeni Z., Foog L.K., A Review: Recent Advances in Ultrasensitive and Highly Specific Recognition Aptasensors with Various Detection Strategies, *RSC Adv.*, **155**: 184–207 (2020).

[32] Jain A.K., Gupta V.K., Sahoo B.B., Singh L.P., Copper(II)-Selective Electrodes Based on Macrocyclic Compounds. *Anal. Proc. Incl. Anal. Commun.*, **32**: 99-101 (1995).

[33] Gupta V.K., Karimi-Maleh H., Sadegh R., Simultaneous Determination of Hydroxylamine, Phenol and Sulfite in Water and Waste Water Samples Using a Voltammetric Nanosensor, *J. Electrochem. Sci.*, **10**: 303-316 (2015).

[34] Jandaghi N., Jahani Sh., Foroughi M.M., Kazemipour M., Ansari M., Cerium-Doped Flower-Shaped ZnO Nano-Crystallites as a Sensing Component for Simultaneous Electrochemical Determination of Epirubicin and Methotrexate, *Microchim. Acta*, **187**: 24-35 (2020).

[35] Gupta V.K., Singh A.K., Kumawat L.K., Thiazole Schiff Base Turn-In Fluorescent Chemosensor for Al^{3+} Ion, *Sens. Actuators B*, **195**: 98-108 (2014).

[36] Srivastava S.K., Gupta V.K., Jain S., PVC-Based 2,2,2-Cryptand Sensors for Zinc Ions, *Anal. Chem.*, **68**: 1272-1275 (1996).

[37] Farvardin N., Jahani Sh., Kazemipour M., Foroughi M.M., The Synthesis and Characterization of 3D Mesoporous Ceo_2 Hollow Spheres as a Modifier for the Simultaneous Determination of Amlodipine, Hydrochlorothiazide and Valsartan, *Anal. Methods*, 12: 1767-1778 (2020).

[38] Gupta V.K., Pathania D., Agarwal S., Sharma S., Decolorization of Hazardous Dye from Water System Using Chemical Modified Ficus Carica Adsorbent, *J. Mol. Liq.*, **174**: 86-94 (2012).

[39] Gupta V.K., Kumar S., Singh R., Singh L.P., Shoora S.K., Sethi B., Cadmium (II) Ion Sensing Through P-Tert-Butyl Calix[6]Arene Based Potentiometric Sensor, *J. Mol. Liq.*, **195**: 65-68 (2014).

[40] Torkzadeh-Mahani R., Foroughi M.M., Jahani Sh., Kazemipour M., Hassani Nadiki H., The Effect of Ultrasonic Irradiation on the Morphology of Nio/CO_3O_4 Nanocomposite and Its Application to the Simultaneous Electrochemical Determination of Droxidopa and Carbidopa, *Ultrason Sonochem.*, **56**: 183-192 (2019).

[41] Karthikeyan S., Boopathy R., Titus A., Sekaran G., A New Approach for the Degradation of High Concentration of Aromatic Amine by Heterocatalytic Fenton Oxidation: Kinetic and Spectroscopic Studies, *J. Mol. Liq.*, **173**: 153-163 (2012).

[42] Dehghani M.H., Sanaei D., Ali I., Bhatnagar A., Removal of Chromium(VI) from Aqueous Solution Using Treated Waste Newspaper as a Low-Cost Adsorbent: Kinetic Modeling and Isotherm Studies, *J. Mol. Liq.*, **215**: 671-679 (2016).

[43] Yaghoubian H., Jahani Sh., Beitollahi H., Tajik S., Hosseinzadeh R., Biparva P., Voltammetric Determination of Droxidopa In The Presence of Tryptophan Using a Nanostructured Base Electrochemical Sensor, *J. Electrochem. Sci. Technol.*, **9**: 109-117 (2018).

[44] Asfaram A., Ghaedi M., Agarwal S., Tyagi I., Gupta V.K., Removal o Basic Dye Auramine-O by ZnS:Cu Nanoparticles Loaded on Activated Carbon: Optimization of Parameters Using Response Surface Methodology with Central Composite Design, *RSC Adv.*, **5**: 18438-18450 (2015).

[45] Gupta V.K., Atar N., Yola M.L., Üstündağ Z., Uzun L., A Novel Magnetic Fe@Au Core–Shell Nanoparticles Anchored Graphene Oxide Recyclable Nanocatalyst for the Reduction of Nitrophenol Compounds, *Water Res.*, **48**: 210-217 (2014).

[46] Rajaei M., Foroughi M.M., Jahani Sh., Shahidi Zandi M., Hassani Nadiki H., Sensitive Detection of Morphine in the Presence of Dopamine with La^{3+} Doped Fern-Like CuO Nanoleaves/ Mwcnts Modified Carbon Paste Electrode, *J.Mol. Liq.*, **284**: 462-472 (2019).

[47] Yola M.L., Gupta V.K., Eren T., Emre Şen A., Atar N., A Novel Electro Analytical Nanosensor Based on Graphene Oxide/Silver Nanoparticles for Simultaneous Determination of Quercetin and Morin, *Electrochim. Acta*, **120**: 204-211 (2014).

[48] Gupta V.K., Mergu V.N., Kumawat L.K., Singh A.K., Selective Naked-Eye Detection of Magnesium(II) Ions Using A Coumarin-Derived Fluorescent Probe, *Sens. Actuators B*, **207**: 216-223 (2015).

[49] Aramesh-Boroujeni Z., Asadi Z., Electrochemical Determination Venlafaxine at Nio/GR Nanocomposite Modified Carbon Paste Electrode, *Iran. J. Chem. Chem. Eng.(IJCCE), Online from May* (2020).
DOI: 10.30492/Ijcce.2020.39188.

[50] Gupta V.K., Mergu N., Kumawat L.K., Singh A.K., A Reversible Fluorescence "Off-On-Off" Sensor for Sequential Detection of Aluminum and Acetate/Fluoride Ions, *Talanta*, **144**: 80-89 (2015).

[51] Karimi-Maleh H., Tahernejad-Javazmi F., Atar N., Yola M.L., Gupta V.K., Ensafi A.A., A Novel DNA Biosensor Based on A Pencil Graphite Electrode Modified with Polypyrrole/Functionalized Multiwalled Carbon Nanotubes for Determination of 6-Mercaptopurine Anticancer Drug, *Ind. Eng. Chem. Res.*, **54**: 3634-3639 (2015).

[52] Iranmanesh T., Jahani Sh., Foroughi M.M., Shahidi Zandi M., Hassani Nadiki H., Synthesis of La_2O_3/MWCNT Nanocomposite as The Sensing Element for Electrochemical Determination of Theophylline, *Anal. Methods*, (2020).
DOI: 10.1039/D0AY01336F.

[53] Jain A.K., Gupta V.K., Singh L.P., Neutral Carrier and Organic Resin Based Membranes as Sensors for Uranyl Ions, *Anal. Proc. Incl. Anal. Commun.*, **32**: 263-265 (1995).

[54] Zhang Y., Zheng J.B., Comparative Investigation on Electrochemical Behavior of Hydroquinone at Carbon Ionic Liquid Electrode, Ionic Liquid Modified Carbon Paste Electrode and Carbon Paste Electrode, *Electrochim. Acta*, **52**: 7210-7216 (2007).

[55] Serpi C., Kovatsi L., Girousi S., Electroanalytical Quantification of Total Dsdna Extracted from Human Sample Using, an Ionic Liquid Modified, Carbon Nanotubes Paste Electrode, *Anal. Chim. Acta*, **812**: 26-32 (2014).

[56] Khatami M., Alijani H., Sharifi I., Sharifi F., Pourseyedi S., Kharazi S., Khatami M.A., Leishmanicidal M., Activity of Biogenic Fe_3O_4 Nanoparticles, *Sci. Pharm.*, **85**: 36-45 (2017).

[57] Kozitsina A.N., Malysheva N.N., Utepova I.A., Glazyrina Y.A., Matern A.I., Brainina KZ., Chupakhin O.N., An Enzyme-Free Electrochemical Method for the Determination of *E. Coli* Using Fe_3O_4 Nanocomposites with a Sio_2 Shell Modified By Ferrocene, *J. Anal. Chem.*, **70**: 540-545 (2015).

[58] Zhang X., Niu J., Zhang X., Xiao R., Lu M., Cai Z., Graphene Oxide-Sio_2 Nanocomposite as the Adsorbent for Extraction and Preconcentration of Plant Hormones for HPLC Analysis, *J. Chromatogr. B*, **1046**: 58-64 (2017).

[59] Beitollahi H., Garkani Nejad F., Shakeri S., GO/Fe_3O_4@SiO_2 Core–Shell Nanocomposite-Modified Graphite Screen-Printed Electrode for Sensitive and Selective Electrochemical Sensing of Dopamine and Uric Acid, *Anal. Methods*, **9**: 5541-5549 (2017).

[60] Bard A.J., Faulkner L.R., "Electrochemical Methods Fundamentals and Applications", 2nd ed., New York: John Wiley & Sons, Inc., (2001).

[61] Fathi S., Omrani S., Zamani S., Simple and Low-Cost Electrochemical Sensor Based on Nickel Nanoparticles for the Determination of Cabergoline, *J. Anal. Chem.*, **71**: 269-275 (2016).

[62] Beitollahi H., Tajik S., Alizadeh R., Nano Composite System Based on ZnO-Functionalized Graphene Oxide Nanosheets for Determination of Cabergoline, *J. Electrochem. Sci. Technol.*, **8**: 307-313 (2017).

[63] Igarashi K., Hotta K., Kasuya F., Abe K., Sakoda S., Determination of Cabergoline and L-Dopa in Human Plasma Using Liquid Chromatography-Tandem Mass Spectrometry, *J. Chromatogr. B*, **792**: 55-61 (2003).

[64] Önal A., Sağırlı O., Şensoy D., Selective LC Determination of Cabergoline in the Bulk Drug and in Tablets: *In Vitro* Dissolution Studies, *Chromatographia*, **65**: 561-567 (2007).